Pergamon

Materials Research Bulletin 37 (2002) 1895–1905

Materials Research Bulletin

Synthesis and crystal structure of two new oxychalcogenides: $Eu_5V_3S_6O_7$ and $La_{10}Se_{14}O$

A. Meerschaut*, A. Lafond, P. Palvadeau, C. Deudon, L. Cario

Laboratoire de Chimie des Solides, Institut des Matériaux Jean Rouxel, UMR 6502 CNRS-Université de Nantes, 2 Rue de la Houssinière, BP 32229, 44322 Nantes Cedex 03, France

(Refereed)
Received 12 April 2002; accepted 23 July 2002

Abstract

The crystal structure determination of two new oxychalcogenides, namely $Eu_5V_3S_6O_7$ and $La_{10}Se_{14}O$, is reported. $Eu_5V_3S_6O_7$ crystallizes in the orthorhombic symmetry (space group *Pmmn*) with unit cell parameters (in Å): $a = 17.463(2)$, $b = 3.6732(4)$, and $c = 10.007(1)$. This compound is isotypic with the $Ln_5V_3S_6O_7$ compounds (Ln = La–Nd), and its structure has been refined to $R1 = 0.0248$. Eu atoms, which are nine-coordinated by O and S atoms, are associated to form ribbons that are interconnected by $[VS_4O_2]$ octahedrons. $La_{10}Se_{14}O$ crystallizes in the tetragonal symmetry (space group $I4_1/acd$) with unit cell parameters (in Å): $a = 15.926(2)$, and $c = 21.061(5)$. The structure was refined to $R1 = 0.0347$. $La_{10}Se_{14}O$ is isostructural with the $Pr_{10}X_{14}O$ compounds (X = S and Se). The only structure difference is observed for one La site that is found split, in connection with a mixed O/Se site filling.

Keywords: A. Oxides/chalcogenides; B. Chemical synthesis; C. X-ray diffraction; D. Crystal structure; D. Electrical properties

1. Introduction

Two-dimensional compounds exhibit very often interesting physical properties related to their low dimensional character such as superconductivity, colossal magnetoresistance, and charge density waves. Although oxychalcogenides were very

* Corresponding author. Tel.: +33-2-40-37-39-17; fax: +33-2-40-37-39-95.
E-mail address: meerschaut@cnrs-imn.fr (A. Meerschaut).

0025-5408/02/$ – see front matter
PII: S0025-5408(02)00883-8

little studied so far, these materials have found a renewed interest since the discovery of new families of layered compounds among them. For example, the doped LaOCuS [1] and $Sr_{n+1}M_nO_{3n-1}Cu_2S_2$ (M = Zn, In, and Ga) [2] compounds that contain $[Cu_2S_2]$ anti-PbO type layers were demonstrated to be interesting p-type transparent conductors. On the other hand, the $Ln_2Ti_2S_2O_5$ [3,4] and $Sr_{n+1}M_nO_{3n-1}Cu_2S_2$ [2,5] compounds contain, respectively, Ti_2O_5 and $Sr_{n+1}M_nO_{3n-1}$ perovskite-type layers that are close to the layers found in cuprates or manganates. It was early noticed by Flahaut and coworkers [6] that very often oxychalcogenide compounds show a composite structure with a segregation of sulfide and oxide layers. This feature makes oxychalcogenide compounds very attractive to find new two-dimensional materials with interesting electronic properties. In that respect, we have started the exploration of several oxychalcogenide systems. During this search we found two new oxychalcogenide compounds, namely $Eu_5V_3S_6O_7$ and $La_{10}Se_{14}O$, which do not have a low dimensional character. This paper is mainly devoted to the structure determination and chemical characterization of these compounds.

2. Experimental

2.1. Synthesis

$Eu_5V_3S_6O_7$ was obtained during an attempt to synthesize an hypothetical composite compound $Eu_3V_2S_3O_5$ built from the stacking of $[Eu_3S_3]$ slabs and defective double perovskite layers $[V_2O_5]$. Powders of EuS (preliminary obtained by sulfurization of EuO under a gas flow of H_2S at 1000°C) and V_2O_5 (Aldrich, 99.9%) were weighed in a 3:1 ratio and finely mixed together. The mixture was loaded into a silica tube sealed under vacuum ($p = 2 \times 10^{-2}$ atm) and heated up at a rate of 10°C h^{-1}, first at 250°C for 1 day, and then to 1050°C for 1 week. The resulting product was then ground and before a second heating cycle a small amount of iodine (<5 mg cm^{-3}) was added to favor crystallization. The final product, inhomogeneous, showed the presence of crystals with a platelet shape (that corresponds to V_5S_8), and few needle shape, black crystals of $Eu_5V_3S_6O_7$.

$La_{10}Se_{14}O$ was obtained as a byproduct during the synthesis from the elements of the misfit bilayer $(LaSe)_{1.14}(NbSe_2)_2$ [7]. A mixture of the elements in the proper ratio was loaded into a silica tube under vacuum ($p = 2 \times 10^{-2}$ atm), and heated up to 1050°C at a rate of 10°C h^{-1}, after 24 h at 250°C. The silica tube was attacked during the heating process and, in the final product, crystals of $La_{10}Se_{14}O$ were found beside those of $(LaSe)_{1.14}(NbSe_2)_2$.

2.2. Data collection

2.2.1. $Eu_5V_3S_6O_7$

A needle-like crystal was mounted on a STOE-IPDS single φ-axis X-ray diffractometer with a two-dimensional area detector based on Imaging Plate technology.

One hundred and fifty-seven images were recorded over the range $0^\circ < \varphi < 220^\circ$ with a φ increment of 1.4°, after an exposure of 12 min for each φ position. The crystal-to-detector distance was set to 70 mm, which authorizes a 2θ range between 3.3 and 52.1°. A total of 5443 reflections were collected, of which 725 were independent with $R(\text{int}) = 0.0804$. Cell parameters were determined from a least-squares analysis of the setting angles of 2819 reflections; this led, in the orthorhombic symmetry, to unit cell values (in Å): $a = 17.463(2)$, $b = 3.6732(4)$, and $c = 10.007(1)$. The structure was solved with the direct method and subsequent difference Fourier calculations using the SHELXS and SHELXL programs [8], respectively. The systematic absences, $h\,k\,0$ with $h + k = 2n + 1$, pointed to two possible space groups. The two choices with the lowest combined figure of merit (CFOM) were $Pm2_1n$ ($P2_1mn$) (acentric, No. 39, CFOM = 6.99), and $Pmmn$ (centric, No. 59, CFOM = 4.48). The intensity statistics rather indicated a centrosymmetric situation (mean $E^2 - 1 = 0.916$; expected 0.968 for centrosymmetric and 0.736 for noncentrosymmetric). Therefore, we proceeded with the $Pmmn$ space

Table 1
Data collection conditions and refinement results for $Eu_5V_3S_6O_7$ and $La_{10}Se_{14}O$

Empirical formula	$Eu_5V_3S_6O_7$	$La_{10}Se_{14}O$
Formula weight, Z	1216.98, 2	2510.50, 8
Crystal habit, color	Needle-like, black	Spherical $r = 0.11$ mm, red
Absorption correction	Faces indexed ($\mu = 27.114$ mm^{-1})	Sphere ($r = 0.11$ mm) (μ =34.74 mm^{-1})
Density	$\rho = 6.297$ g cm^{-3}	$\rho = 6.251$ g cm^{-3}
Diffractometer	STOE-IPDS	Enraf-Nonius CAD4
Radiation	Mo Kα ($\lambda = 0.7107$ Å)	Mo Kα ($\lambda = 0.7107$ Å)
Crystal-to-detector distance, θ range	70 mm, $2.20^\circ \le \theta \le 25.870^\circ$	–, $2.560^\circ \le \theta \le 34.960^\circ$
Indices range collection ($h\,k\,l$)	−21, 21; −4, 4; −12, 12	−25, 25; 0, 25; 0, 33
Refinement results		
Cell parameters (Å)	$a = 17.463(2)$, b =3.6732(4), $c = 10.007(1)$	$a = b = 15.926(2)$, c =21.061(5)
Symmetry	Orthorhombic	Tetragonal
Space group	$Pmmn$ (No. 59)	$I4_1/acd$ (No. 142)
Independent reflections	725 [R(int) = 0.0783]	2864 [R(int) = 0.0887]
Absorption correction, T_{min}/T_{max}	0.6046/0.7682	0.0135/0.0407
Refinement method	Full-matrix least-squares on F^2, SHELXL	Full-matrix least-squares on F^2, JANA2000
Data, parameters	725, 48	2864, 62
Goodness-of-fit on F^2	0.836	2.56
Reliability factors $R1$ (all reflections)	0.0458	0.0538
Reliability factors $R1$; $wR2$	0.0248; 0.0369 (538 reflections with $I \ge 2\sigma(I)$)	0.0347; 0.0416(2120 reflections with $I \ge 3\sigma(I)$)
Largest peaks in Fourier difference (e$^-$ Å^{-3})	+1.43; −1.83	+2.95; −5.17

$R1 = \sum(|F_{obs}| - |F_{calc}|)/\sum(F_{obs})$; $wR2 = (\sum w(|F_{obs}| - |F_{calc}|)^2/\sum w(F_{obs})^2)^{1/2}$; $w = 1$.

Table 2a
Atom coordinates and isotropic temperature parameters (or U_{eq}^*) ($Å^2 \times 10^4$)

Atom	Site	x	y	z	U_{iso}, U_{eq}^*
Eu1	4f	0.63650(3)	1/4	0.46922(7)	47(2)*
Eu2	2a	3/4	−1/4	0.72611(9)	42(2)*
Eu3	4f	0.58603(3)	−1/4	0.08472(6)	47(2)*
V1	4f	0.5558(1)	−1/4	0.7466(2)	45(5)*
V2	2b	3/4	1/4	0.1843(3)	47(7)*
S1	2a	3/4	−1/4	0.3580(5)	61(10)
S2	4f	0.4820(2)	1/4	0.6458(3)	52(7)
S3	2a	3/4	−1/4	1.0312(5)	42(8)
S4	4f	0.6331(2)	−3/4	0.8549(3)	40(6)
O1	2b	3/4	−3/4	0.5941(12)	29(22)
O2	4f	0.6292(5)	−1/4	0.6061(8)	86(19)
O3	4f	0.4962(4)	−1/4	0.9005(8)	46(18)
O4	4f	0.6476(5)	1/4	0.2078(8)	86(19)

U_{eq}^* is defined as one third of the trace of the orthogonalized U_{ij} tensor.

group. Intensities were corrected for absorption effects ($\mu = 27.11\ mm^{-1}$) using the faces indexed option. The crystal was idealized as a parallelepiped with dimensions 0.008 mm × 0.12 mm × 0.005 mm, bounded by faces {1 0 0}, {0 1 0}, and {0 0 1}, respectively; minimum and maximum transmission factors were 0.6046 and 0.7682. In the final stages of refinement, i.e. with Eu and V atoms refined anisotropically, the reliability factors converged to $R1 = 0.0248$ and $wR2 = 0.0369$ for 538 reflections with $F_o > 4\sigma(F_o)$ and 48 parameters ($R1 = 0.0458$ for all data (=725)). The maximum and minimum peaks on the final Fourier difference map corresponded to 1.43 and $-1.83\ e^-\ Å^{-3}$, respectively. Details on data collection and structure refinements are given in Table 1. The atomic positions and equivalent isotropic displacement parameters are given in Table 2a; coefficients of the anisotropic displacement parameters for Eu and V are reported in Table 2b. Selected bond lengths (coordination polyhedron of the Eu and V atoms) are given in Table 3.

2.2.2. $La_{10}Se_{14}O$

A sphere-like crystal was mounted on an Enraf-Nonius CAD4 diffractometer using graphite monochromatized Mo Kα radiation ($\lambda = 0.71073$ Å). Intensities were collected within the theta range 2.6–35° with the θ–2θ technique. After averaging

Table 2b
Coefficients of the anisotropic temperature factors for $Eu_5V_3S_6O_7$

Atom	U_{11}	U_{22}	U_{33}	U_{12}	U_{13}	U_{23}
Eu1	0.0059(3)	0.0017(4)	0.0065(3)	0	−0.0008(3)	0
Eu2	0.0056(4)	0.0018(6)	0.0054(5)	0	0	0
Eu3	0.0055(3)	0.0026(4)	0.0060(3)	0	0.0002(3)	0
V1	0.0021(9)	0.0077(13)	0.0037(11)	0	0.0012(9)	0
V2	0.0029(13)	0.0052(20)	0.0059(16)	0	0	0

Table 3
Selected bond lengths (Å) for $Eu_5V_3S_6O_7$

	Bond lengths (Å)	SO[a]
Eu1-polyhedron		
O2 (×2)	2.295(5)	#1
O1	2.343(6)	#1
O4	2.623(8)	
S2 (×2)	2.922(2)	#1
S2 (×2)	2.997(2)	#2, #3
S2	3.225(3)	
Eu2-polyhedron		
O1 (×2)	2.262(7)	#1
O2 (×2)	2.428(8)	#4
S4 (×4)	3.033(2)	#1, #4, #5
S3	3.053(5)	
Eu3-polyhedron		
O3 (×2)	2.336(4)	#2, #7
O3	2.421(8)	#8
O4 (×2)	2.459(5)	#6
S3	2.913(1)	#8
S2	2.946(3)	#2
S4 (×2)	3.056(2)	#8, #9
V1-polyhedron		
O3	1.859(8)	
O2	1.902(8)	
S2(×2)	2.460(3)	#6
S4(×2)	2.524(3)	#1
Eu1–V distances		
V2	3.472(2)	
V1 (×2)	3.614(2)	#1
Eu2–V distances		
V1 (×2)	3.397(2)	#4
Eu3–V distances		
V1	3.425(2)	#8
V1 (×2)	3.515(2)	#2, #7
V2	3.5447(10)	#11
V2-polyhedron		
04(×2)	1.804(9)	#11
S3 (×2)	2.392(4)	#8, #9
S1 (×2)	2.528(4)	#1

[a] SO symmetry operations used to generate equivalent atoms—#1: x,$y+1$,z; #2: $-x+1$,$-y$,$-z+1$; #3: $-x+1$,$-y+1$,$-z+1$; #4: $-x+3/2$, $-y-1/2$,z; #5: $-x+3/2$,$-y-3/2$,z; #6: x,$y-1$,z; #7: $-x+1$,$-y-1$,$-z+1$; #8: x,y,$z-1$; #9: x,$y+1$,$z-1$; #10: x,y,$z+1$; #11: $-x+3/2$,$-y+1/2$,z.

($R(\text{int}) = 0.0887$), a total of 2864 reflections was kept for the refinement. Intensities were corrected for absorption effects ($\mu = 34.74\ \text{mm}^{-1}$) considering the crystal as a regular sphere of diameter $r = 0.11$ mm; minimum and maximum transmission factors were 0.0135 and 0.0407, respectively. The unit cell parameters were

determined from a least-squares refinement using 25 well-centered reflections with the CELLDIM program ($14^\circ < 2\theta < 36^\circ$). In the tetragonal symmetry, the resulting cell dimensions (in Å): $a = b = 15.926(2)$, and $c = 21.061(5)$. The existing conditions for the observed reflections led to the unique space group $I4_1/acd$ (No. 142). The structure was solved with the direct method and subsequent difference Fourier calculations. Refinement with all atoms (three La, four Se, and one O) and isotropic thermal parameters, using JANA2000 program [9], converged to reliability factors $R1 = 0.0644$ for 2120 reflections ($I > 3\sigma(I)$) and $R1 = 0.0853$ for all data (2864 reflections) with 27 parameters. At this stage, the B value for oxygen was negative. A refinement taking into account anisotropic displacement parameters for both La and Se atoms improved the R factors: $R1 = 0.0391$, $R1\,(\text{all data}) = 0.0586$, but the B value for O remained negative. A difference Fourier calculation at this stage revealed a large residual peak of 9.46 e^- Å^{-3} (the second one at 2.76 e^- Å^{-3}), at 0.62 Å from La2. This led us to consider the splitting of the La2 position into two sites (La2 and La21), with the constraint that the sum of their occupancy is 100% and their U_{eq} parameters identical. Correlatively, we also considered a mixed occupancy between O and Se on the oxygen position, with the constraint that the proportion of O/Se in this mixed site is the same as the proportion of La2/La21 for the split position. Under these

Table 4a
Atom coordinates and isotropic temperature parameters (or U_{eq}) (Å$^2 \times 10^4$)

Atom	Site	s.o.f.	x	y	z	U_{iso}, U_{eq}*
La1	32g	1	0.12959(2)	0.02711(2)	0.04709(1)	95(1)*
La2	32g	0.945(3)	0.37021(5)	0.25469(2)	0.05951(2)	103(1)*
La21	32g	0.055(–)	0.3457(8)	0.2583(4)	0.0486(4)	103(–)*
La3	16f	1	0.13383(2)	$x + 1/4$	3/8	90(1)*
Se1	32g	1	0.02262(3)	0.38140(3)	0.00165(2)	124(1)*
Se2	32g	1	0.34210(3)	0.07100(3)	0.09265(2)	118(1)*
Se3	32g	1	0.03890(3)	0.07120(3)	0.17153(2)	105(1)*
Se4	16e	1	0.35436(4)	0	1/4	99(2)*
O	8a	0.945(–)	0	1/4	3/8	54(10)
Se5	8a	0.055(–)	0	1/4	3/8	54(–)

s.o.f.; site occupancy factor.

Table 4b
Coefficients of the anisotropic temperature factors for $La_{10}Se_{14}O$

Atom	U_{11}	U_{22}	U_{33}	U_{12}	U_{13}	U_{23}
La1	0.0139(1)	0.0097(1)	0.0049(1)	0.001(1)0	0.00062(9)	0.00035(9)
La2/21	0.0123(2)	0.0099(1)	0.0086(1)	−0.0018(1)	−0.0000(2)	0.0009(1)
La3	0.0103(1)	0.0103(–)	0.0065(2)	0.0004(2)	−0.0005(1)	$-U_{13}$
Se1	0.0119(2)	0.0132(2)	0.0120(2)	0.0023(2)	0.0020(2)	−0.0017(2)
Se2	0.0196(2)	0.0097(2)	0.0062(2)	0.0012(2)	0.0036(2)	0.0007(2)
Se3	0.0099(2)	0.0148(2)	0.0069(2)	−0.0006(2)	0.0012(2)	0.0002(2)
Se4	0.0107(3)	0.0121(3)	0.0068(2)	0	0	0.0002(2)

conditions, the final cycle of least-squares refinement on F_0^2 resulted in values $R1 = 0.0347, R1\,(\text{all}) = 0.0538$, for 62 variables. The maximum and minimum peaks on the final Fourier difference map corresponded to 2.95 (less than 1% of an La atom) and $-5.17\,e^-\,Å^{-3}$, respectively. The atomic positions and equivalent isotropic displacement parameters are given in Table 4a; coefficients of the anisotropic

Table 5
Selected bond lengths (Å) for $La_{10}Se_{14}O$

	Bond lengths (Å)	SO[a]
La1-polyhedron		
Se1	2.9859(6)	#2
Se1	3.0563(7)	#3
(Se2)	(3.5868(7))	#1
Se2	3.0585(6)	#4
Se2	3.1011(6)	#5
Se3	3.0737(6)	#1
Se3	3.1043(6)	#5
Se4	3.0076(6)	#6
La3-polyhedron		
Se1	3.1444(6)	#1
Se1	3.1444(6)	#10
Se2	3.0818(6)	#8
Se2	3.0818(6)	#11
Se3	3.0069(6)	#2
Se3	3.0069(6)	#5
Se4	3.2233(2)	#9
Se4	3.2233(2)	#8
La2-polyhedron		
(Se1)	(3.4998(9))	#7
Se1	2.9402(8)	#4
Se2	3.0406(7)	#1
Se2	3.2884(8)	#8
Se3	3.0881(8)	#6
Se3	3.1519(10)	#5
Se4	3.2056(8)	#8
O	2.4860(8)	#9
La21-polyhedron		
Se1	3.059(11)	#4
Se2	3.125(8)	#1
Se2	3.330(9)	#8
Se3	2.804(10)	#6
Se3	2.834(13)	#5
S4	2.855(10)	#8
Se5	2.942(12)	#9

[a] SO, symmetry operations used to generate equivalent atoms—#1: x,y,z; #2: $-x,1/2-y,z$; #3: $x,-1/2+y,-z$; #4: $1/2-x,y,-z$; #5: $1/4-y,1/4-x,1/4-z$; #6: $1/4+y,1/4-x,\ -1/4+z$; #7: $1/2+x,1/2-y,-z$; #8: $1/4+y,3/4-x,1/4-z$; #9: $1/2-x,1/2-y,1/2-z$; #10: $-1/4$.

displacement parameters for La and Se are reported in Table 4b. Selected bond lengths (coordination polyhedron of the La and Se atoms) are given in Table 5.

3. Results and discussions

Fig. 1 shows the projection of the structure of $Eu_5V_3S_6O_7$ onto the (a,c) plane. The structure of $Eu_5V_3S_6O_7$ is isotypic with the $Ln_5V_3S_6O_7$ (Ln = La–Nd) series of compounds mentioned by Dugué et al. [10]. One observes that Eu atoms are nine-fold coordinated with O and S atoms in a tricapped trigonal prisms: (i) Eu1 resides in a trigonal prism Eu1-$(S1)_2(S2)_2(O2)_2$ with two capping O1 and O4 atoms and one capping S2 atom; (ii) Eu2 in a trigonal prism Eu2-$2(S4)_2(O1)_2$ with two capping O2 atoms and one capping S3 atom; and (iii) Eu3 in a trigonal prism Eu3-$(S4)_2(O3)_2(O4)_2$ with two capping S2 and S3 atoms and one O3 atom. The main interatomic distances within each centered Eu-polyhedron are reported in Table 3. Two adjacent Eu3-polyhedrons are connected through their common triangular face ($3 \times O3$) to form a double Eu-ribbon parallel to b, while Eu1- and Eu2-polyhedrons are associated together to form a triple Eu-ribbon parallel to b. These different Eu associations are interconnected by discrete $[VS_4O_2]$ octahedrons (see Fig. 2a). Such a

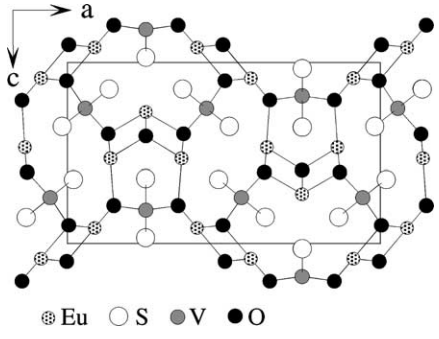

Fig. 1. Projection of the structure of $Eu_5V_3S_6O_7$ onto the (a,c) plane.

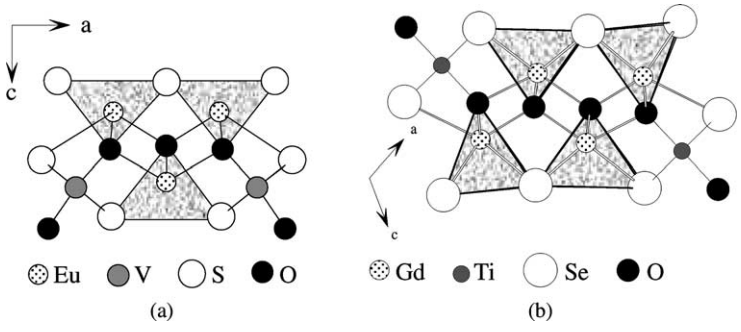

Fig. 2. (a) Structure fragment constituted by the association of three Eu-polyhedrons in $Eu_5V_3S_6O_7$. (b) Elemental building block of the $Gd_4TiSe_4O_4$ compound.

building principle was already put forward in the structure description of $Gd_4TiSe_4O_4$ [11]. Indeed, in this compound, association of four (instead of three or two) adjacent Gd-polyhedrons constituted the elemental building unit which develops into ribbons along *b*; these entities are also interconnected through discrete $[TiSe_4O_2]$ octahedrons on both end sides (see Fig. 2b). The structure fragment resulting from the condensation of three or four Ln-polyhedrons can be extended to the infinity as exemplified in $La_4Se_3O_4$ [12], leading to $[Ln_2O_2]$ slabs that are interleaved by planar Se sheets. In such a case, there is no interconnecting $[TX_4O_2]$ octahedron. In many examples of two-dimensional composite compounds, such an $[Ln_2O_2]$ organization is often encountered (see LaOCuS [1], or $La_2Fe_2O_3Se_2$ [13], where $[La_2O_2]$ slabs alternate with $[Fe_2OSe_2]$ slabs).

One interesting feature of $Eu_5V_3S_6O_7$ is related to the oxidation state of vanadium. If we assume Eu^{3+}, S^{2-}, and O^{2-} to be the normal oxidation states in $Eu_5V_3S_6O_7$, we need to consider a mixed valence state for vanadium ($2V^{4+}$ and $1V^{3+}$) in order to reach a charge balance. According to the V^{4+}/V^{3+} ratio 2/1 that matches the ratio of the site multiplicity of V1 and V2 atoms, it is tempting to assign the V^{4+} state to the V1 atom (4f site), and the V^{3+} state to the V2 atom (2b site). This assumption is not supported by bond valence calculations using the equation reported by Brese and O'Keefe [14]: $v_{ij} = \exp[(R_{ij} - d_{ij})/b]$ (where $b = 0.37$, R_{ij} are tabulated values (V–O and V–S), and d_{ij} are the experimental interatomic distances), which leads to bond valence values of 3.5 for V1 and 4.0 for V2. As the mixed valence state of vanadium could be associated to interesting electronic properties, we have performed a four probe conductivity measurements for one $Eu_5V_3S_6O_7$ needle-like crystal between 297 and 150 K. The measured resistance follows an activation law as demonstrated in Fig. 3. In fact, $Eu_5V_3S_6O_7$ behaves as a normal semiconductor with a band gap of the order of 0.2 eV.

Fig. 4 shows the projection of the structure of $La_{10}Se_{14}O$ onto the (*a*,*a*) plane; $La_{10}Se_{14}O$ is isostructural with the $Pr_{10}X_{14}O$ compounds ([15] for X = S,

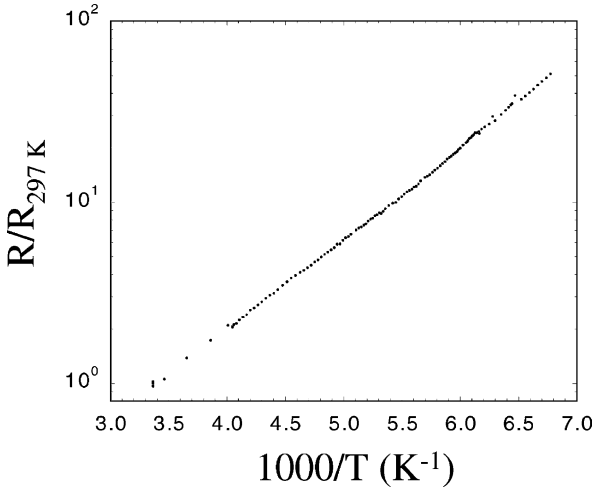

Fig. 3. Normalized resistivity $R/R_{297\ K}$ vs. 1000/T for $Eu_5V_3S_6O_7$.

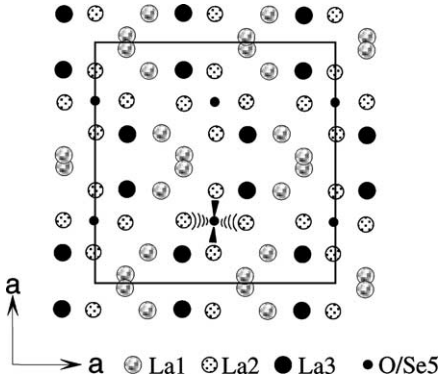

Fig. 4. Projection of the structure of $La_{10}Se_{14}O$ onto the (a,a) plane.

and [16] for X = Se). In this very complex structure, La atoms have either a coordination number of seven (let say 7 + 1) (La1 and La2/La21) or eight (La3); the seven shortest La21–Se bonds are less well known, because of the closeness of La21 to La2, and are in the range 2.80–3.33 Å, compared to a range of 2.94 to 3.29 Å for La1, La2, and La3. For the seven coordinated La atoms, two larger La–Se distances ($\geq$3.5 Å) are present (see Table 5: La1–Se2 and La2–Se1); the very long La21–Se5 distance of 3.742 Å means that Se5 is not in the coordination sphere of La21. The main difference with the previous structure determinations concerns the findings of both the split La2 position, and correlatively the mixed O/Se5 site; this situation means a lower oxygen content than previously refined (oxygen nonstoichiometry), but also that La21 is only present when Se5 is present (see Fig. 5), with a normal bond length La21–Se5 of 2.942 Å. The oxygen deficiency, and consequently the O/Se substitution was first revealed by the negative B value which became positive after taking into account a mixed O/Se site filling. The experimentally derived stoichiometry is thus $La_{10}Se_{14.06}O_{0.94}$, which gives credit to the existence of the solid solution $Ln_{10}S_{15-x}O_x$ earlier reported (as illustrated by the example of $La_{10}S_{14.5}O_{0.5}$ [17]). This O/Se substitution does not alter the charge equilibrium if one considers

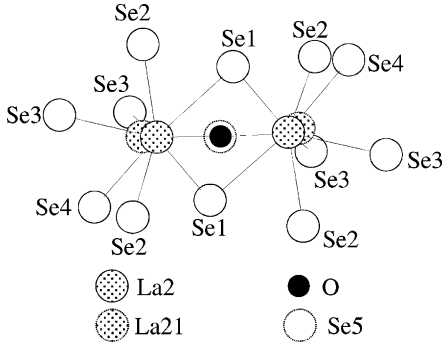

Fig. 5. Coordination sphere around La2/La21 atoms and their interconnection.

La^{3+}, Se^{2-}, and O^{2-}. As already mentioned [15–17], oxygen atom is tetrahedrally coordinated with La2 atoms only (see Fig. 4). The connection between two adjacent La2-polyhedrons is shown in Fig. 5.

To conclude, we have characterized two new oxychalcogenide compounds, namely $Eu_5V_3S_6O_7$ and $La_{10}Se_{14}O$. $Eu_5V_3S_6O_7$ is a new member of the $Ln_5V_3S_6O_7$ family of compounds first reported by Dugué et al. [10] for Ln = La–Nd. This compound shows a semiconducting behavior ($E_g \approx 0.2$ eV). $La_{10}Se_{14}O$ is a new member of the large family of compounds $Ln_{10}X_{14}O$ (Ln = rare earth; X = S and Se). Compared to previous structure determinations [15–17], we found that one La site is split in correlation with a mixed O/Se site filling.

References

[1] M. Palazzi, C.R. Acad. Sci. Paris 292 (Série II) (1981) 789–791;
K. Ueda, S. Inoue, S. Hirose, H. Kawazoe, H. Hosono, Appl. Phys. Lett. 77 (2000) 2701.
[2] W.J. Zhu, P.H. Hor, J. Solid State Chem. 130 (1997) 319–321;
K. Ueda, S. Hirose, H. Kawazoe, H. Hosono, Chem. Mater. 13 (2001) 1880–1883.
[3] M. Goga, R. Seshadri, V. Ksenofontov, P. Gütlich, W. Tremel, Chem. Commun. (1999) 979–980.
[4] C. Boyer, C. Deudon, A. Meerschaut, C.R. Acad. Sci. Paris t2 (Série IIc) (1999) 93–99.
[5] K. Otzschi, H. Ogino, J.-I. Shimoyama, K. Kishio, J. Low Temp. Phys. 117 (1999) 729–733.
[6] M. Guittard, S. Bénazeth, J. Dugué, S. Jaulmes, M. Palazzi, P. Laruelle, J. Flahaut, J. Solid State Chem. 51 (1984) 227–238.
[7] R. Roesky, A. Meerschaut, J. Rouxel, Z. Anorg Allg. Chem. 619 (1993) 117–122.
[8] G.M. Sheldrick: SHELXTL version 5. An integrated system for solving, refining and displaying crystal structure from diffraction data. Siemens Analytical X-ray Instruments Inc., Madison, WI, USA, 1996.
[9] V. Petricek, M. Dusek, Jana2000: a structure refinement chain program for modulated and composite structure, Acad. Sci. Czech Republic, Praha (2000).
[10] J. Dugué, T. Vovan, P. Laruelle, Acta Crystallogr. C41 (1985) 1146–1148;
T. Vovan, J. Dugué, M. Guittard, C.R. Acad. Sci. Paris t292 (1981) 957–959.
[11] A. Meerschaut, A. Lafond, V. Meignen, C. Deudon, J. Solid State Chem. 162 (2001) 182–187.
[12] J. Dugué, D.C. Adolphe, P. Khodadad, Acta Crystallogr. B26 (1970) 1627.
[13] J.M. Mayer, L.F. Schneemeyer, T. Siegrist, J.V. Waszczak, B. van Dover, Angew. Chem. Int. Ed. Engl. 4621 (1992) 14101.
[14] N.E. Brese, M. O'Keefe, Acta Crystallogr. B47 (1991) 192–197.
[15] D. Carré, P. Laruelle, P. Besançon, C.R. Acad. Sci. Paris C270 (1970) 537–539.
[16] F.A. Weber, T. Schleid, Z. Anorg. Allg. Chem. 627 (2001) 1383–1388.
[17] P. Besançon, D. Carré, P. Laruelle, Acta Crystallogr. B29 (1973) 1064–1066.